

YAG:Ce³⁺ nanostructured particles obtained *via* spray pyrolysis of polymeric precursor solution

L. Mancic^{a,*}, K. Marinkovic^a, B.A. Marinkovic^b, M. Dramicanin^c, O. Milosevic^a

^a Institute of Technical Sciences of Serbian Academy of Sciences and Arts, Knez Mihailova 35/IV, 11000 Belgrade, Serbia

^b Departamento de Ciência dos Materiais e Metalurgia, Pontifícia Universidade Católica do Rio de Janeiro, Gávea 22453-900, Rio de Janeiro, Brazil

^c Institute of Nuclear Sciences “Vinca”, PO Box 522, 11001 Belgrade, Serbia

Available online 26 June 2009

Abstract

Cerium-doped yttrium aluminum garnet (YAG:Ce³⁺) powder phosphor is synthesized *via* spray pyrolysis of polymeric precursor solution obtained by dissolving the corresponding nitrates in ethylenediaminetetraacetic acid (EDTA). Ultrasonically generated aerosol droplets are decomposed at 600 °C in argon atmosphere. Following the initial attempt in providing pure YAG:Ce³⁺ phase generation the particles were additionally thermally treated for 3 h in air at 1000 and 1100 °C. The powder morphology is followed with scanning electron microscopy (SEM), while inner particle structure is analysed by analytical and high-resolution transmission electron microscopy (TEM). Phase identification is performed by X-ray powder diffraction (XRPD) based on which a structural refinement through Rietveld method was done. The spherical submicronic particles have grained sub-structure comprising clustered garnet monocrystals sized below 100 nm. The YAG:Ce³⁺ emission shows wide peak in the range 470–600 nm with the maximum near 520 nm.

© 2009 Elsevier Ltd. All rights reserved.

Keywords: B. X-ray methods; Spray pyrolysis; Polymeric precursor; Garnet

1. Introduction

Garnet phase of yttrium aluminum system (Y₃Al₅O₁₂—YAG) represents a good host material for rare earth based phosphors. Owing to its good thermal stability and excellent optical and mechanical properties it has been widely used in optoelectronic devices.^{1–3} When is doped with Ce³⁺, it represents a commercial white pc-LEDs (liquid crystal displays), since Ce³⁺ in YAG efficiently absorbs blue light from 450 to 470 nm and emits a broad band of luminescence in the range of 510 nm to over 600. The key for the further development of high-resolution displays which can achieve superior luminescence performance requires the development of the synthesis method that leads to the formation of pure and ultrafine particles. Synthesis of commercial YAG phosphors is usually done through solid state reaction between the corresponding oxides. Pure YAG phase is hard to achieve due to the fact that Y₂O₃–Al₂O₃ is a complex system that has two more intermediate compounds

with the following composition: perovskite YAlO₃ (YAP) and monoclinic Y₄Al₂O₉ (YAM).⁴ Therefore much effort has been invested in finding a way of synthesizing pure YAG phase through wet-chemical methods.^{5–7} Syntheses from the aerosol are found to be of great value since result in well-defined powder characteristics,^{8–10} essential for achieving higher brightness and resolution in displays. Particularly, spray pyrolysis is one of the simplest among them and is capable in ensuring particle spherical morphology, good crystallinity and uniformity in size and shape. Those characteristics enhance uniform distribution of the luminescent centre in the host matrix influencing final luminescence properties.^{1,2} Recently, we have presented the processing of spherical, uniformly sized nanostructured YAG:Ce³⁺ particles *via* spray pyrolysis of aqueous nitrates solutions at 900 °C.¹¹ However, the control over their morphological properties is not completely achieved due to the fact that fully dense particles were not formed. Additionally, applying the concept of low-temperature aerosol decomposition results in preservation of the desired powder morphology but formation of YAG phase is still followed by YAM, Y₂O₃ and Al₂O₃ mixture.¹² The drawback is in the fact that high-heating rates and short residence time inherent to spray pyrolysis process lead to the

* Corresponding author.

E-mail address: lidija.mancic@itn.sanu.ac.rs (L. Mancic).

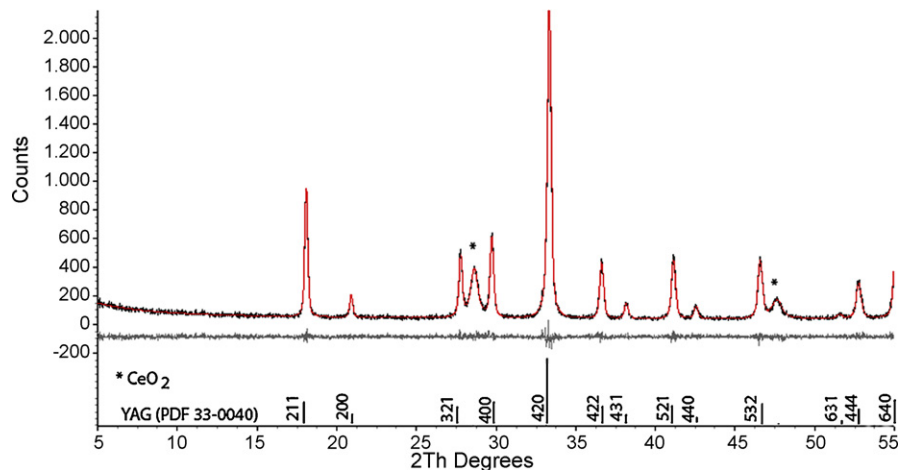


Fig. 1. Rietveld refinement of X-ray diffraction pattern of YAG:Ce³⁺ powder obtained *via* spray pyrolysis and thermally treated at 1000 °C.

formation of kinetically stable phases rather than the thermodynamically stable target YAG phase.⁸ Since spray pyrolysis offers different approaches for controlling of the particle morphology and composition, here obtaining of the YAG:Ce³⁺ particles with spherical and filled morphology were done through introduction of polymeric precursor solutions. The concept of polymeric precursor in spray pyrolysis has been applied in ZrO₂¹³ and YBa₂Cu₃O₇ systems.¹⁴ Formation of precursor solution is based on the idea to form a mixture of cations in an organic complexing agent (EDTA) and ethylene glycol (EG) solution. Two reactions are involved, a complex formation between EDTA and metals (*via* four carboxylate and two amine groups) and esterification between EDTA and EG.¹⁴ Synthesis of YAG through classical EDTA route has been previously reported, but porous polycrystalline powders were obtained through subsequent calcination process.⁵ We report here, for the first time, using of this route in spray pyrolysis with the attempt to confine the polymerization process within a droplet in order to prevent cation segregation on the larger scale, ensure the needed spherical and solid particle morphology and enable formation of YAG:Ce³⁺ phase.

Table 1
The Rietveld refinement details and corresponding reliability factors for YAG:Ce³⁺.

	1000 °C	1100 °C
Space group	<i>Ia-3d</i>	<i>Ia-3d</i>
<i>a</i> (Å)	12.0267(7)	12.0275(7)
Bond distance (Å)		
Y–O ₂	2.311	2.311
Y–O ₁	2.442	2.442
Y–Al	3.006	3.006
Crystallite size (nm)	52(2)	69(3)
Microstrain (%)	0.27(2)	0.21(2)
<i>R</i> _{Bragg} (%)	1.271	1.577
<i>R</i> _{wp} (%)	11.117	12.657
Goodness-of-fit	1.139	1.222

YAG¹⁸: unit cell *a* = 12 Å, bond distance (Å): Y–O₂ = 2.303; Y–O₁ = 2.432; Y–Al = 3.002.

2. Experimental method

Precursor solution for YAG:Ce³⁺ synthesis is prepared through route proposed by Wang et al.⁵ Mixing of yttrium and aluminum nitrates is done at the stoichiometric YAG phase ratio, Y:Al = 3:5. Quantity of cerium nitrate added to the solution cor-

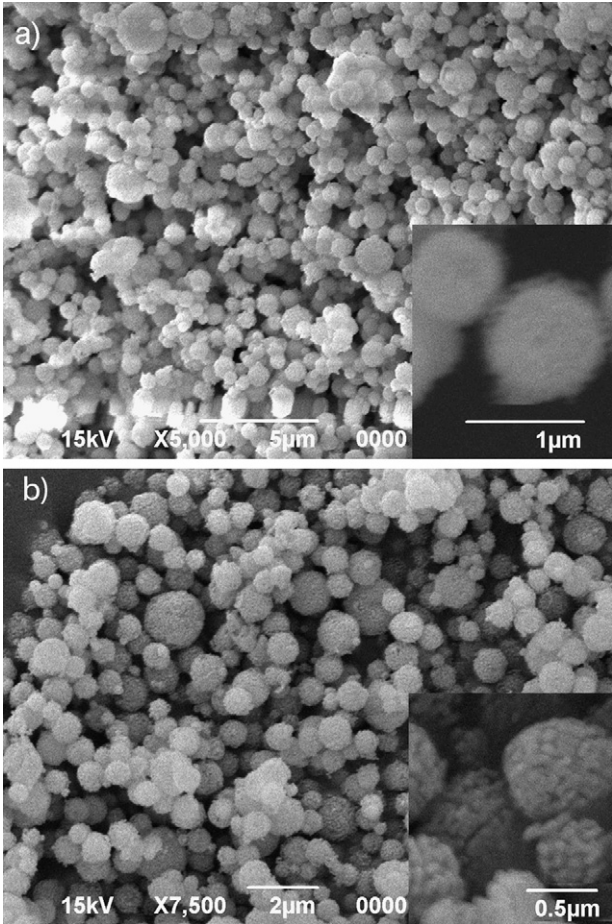


Fig. 2. SEM micrographs of YAG:Ce³⁺ powders annealed at 1000 °C (a) and 1100 °C (b).

responded to 2 at% doping concentration. Contents of EDTA and EG are kept to be: EDTA towards metal ions of 1 and EG/EDTA = 4. First EDTA is dissolved in ammonium hydroxide at 60 °C. The solution is then heated at 80 °C and EG is added. A clear solution with pH value of 5 is formed. Metal nitrate aqueous solutions, separately prepared, are then drop-wise added to the main solution. The pH value is kept at 5 by continuous addition of NH_4OH thus preventing the EDTA precipitation. When all the metal nitrates were complexed, pH value was corrected by HNO_3 addition. Final precursor solution atomized at 1.3 MHz has the following characteristics: concentration $c = 0.12 \text{ mol/dm}^3$, pH 0.15, density $\rho = 0.12485 \text{ g/cm}^3$ and surface tension $\gamma = 64.2 \text{ mN/m}$. Based on these values, the average droplet size¹⁵ and the mean particle size¹⁶ are calculated as to be $3.22 \text{ }\mu\text{m}$ and 991 nm . As-formed aerosol is fed into a triple-zone tubular quartz reactor by the laminar flow of argon gas

($1 \text{ dm}^3/\text{min}$). Temperature zones in the furnace are set at 400, 600 and 600 °C, respectively. The as-prepared powder, black in colour (indicating organic residue) is collected and thermally treated at 1000 and 1100 °C for 3 h. Thermally treated powders, white in colour, were then used for further characterization.

X-ray diffraction analysis (XRD) using a Bruker D-5000, operating with $\text{Cu K}\alpha$ radiation at 30 mA and 40 kV is used to identify the phases in the system. Microstructural data were obtained through Rietveld refinement performed by Topas Academic software.¹⁷ The Rietveld method is a powerful method for the extraction of structural information from powder diffraction patterns. In the Rietveld analysis the least squares refinements method are carried out until the best fit is obtained between the calculated patterns, which is based on the refined structure models, and the observed diffraction pattern. Rietveld refinements were performed using the Topas software in which the

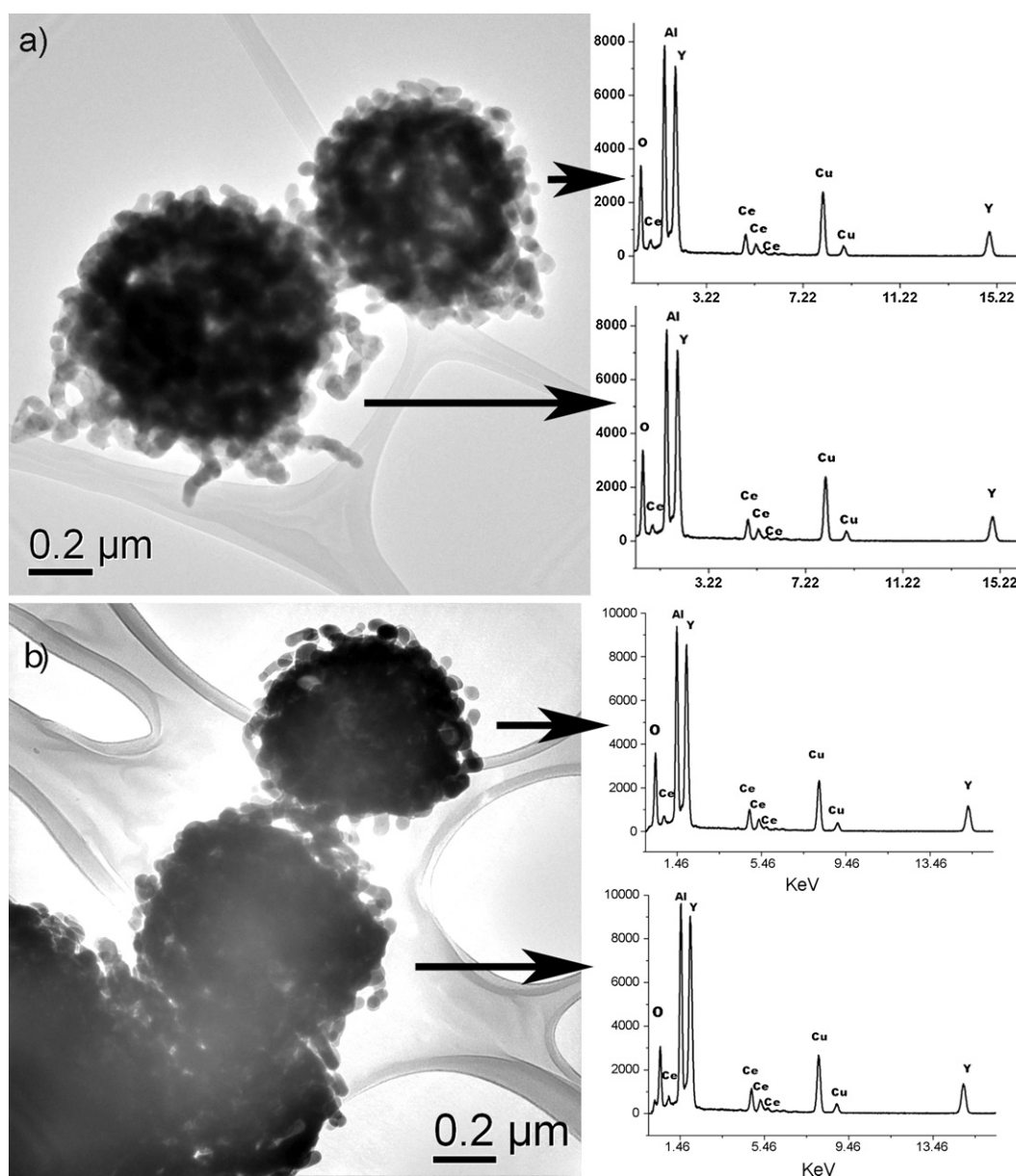


Fig. 3. TEM micrographs of YAG:Ce^{3+} powders heat treated at 1000 °C (a) and 1100 °C (b) with corresponding EDS analyses.

FWHM based LVol (volume weighted mean column height) calculation is used to determine intermediate crystallite size broadening modelled by a Voigt function, while FWHM based strain calculation is used assuming purely Lorentzian-type strain broadening. Powder morphology is observed *via* scanning electron microscopy SEM JEOL JSM-6390-LV. Transmission electron microscopy (TEM) images are recorded using a Gatan CCD camera on a JEOL-2010 microscope operating at 200 kV. While high-resolution transmission electron microscopy combined with Fast Fourier Transformation (FFT) is conducted for accomplishing of the particle crystal structure, their chemical compositions were examined *via* energy dispersive X-ray spectroscopy (EDS). Optical properties are measured at room temperature by a spectrofluorometer system Fluorolog-3 Model

FL3-221 (HORIBA JOBIN-Yvon). A xenon lamp (450 W) is used for excitation of phosphor particles in the UV region.

All the measurements for precursor characterization are done at 20 °C employing the following equipment: pH value – Orion research pH/milivoltmeter 611, density – AP-PAAR density meter DMA 55, surface tension – digital tensiometer K10T Kruss.

3. Results and discussion

Fig. 1 illustrates Rietveld refinement of the X-ray diffraction pattern related to the product obtained after the thermal treatment at 1000 °C (3 h). It suggests that garnet phase was formed without contamination of other phase having different aluminum yttrium composition. The position and the intensities of peaks in the bottom line at Fig. 1 correspond to YAG cubic structure, space group $Ia-3d$ (PDF 33-0040). The refinement details and reliability factors obtained through Rietveld analysis are given in Table 1, together with the unit cell parameters and structural data. Increase of the unit cell parameters and bond lengths are indicative in both cases implying that Y^{3+} (90 pm) is partially substituted by bigger Ce^{3+} (102 pm). However, an incomplete substitution is evident due to the detection of

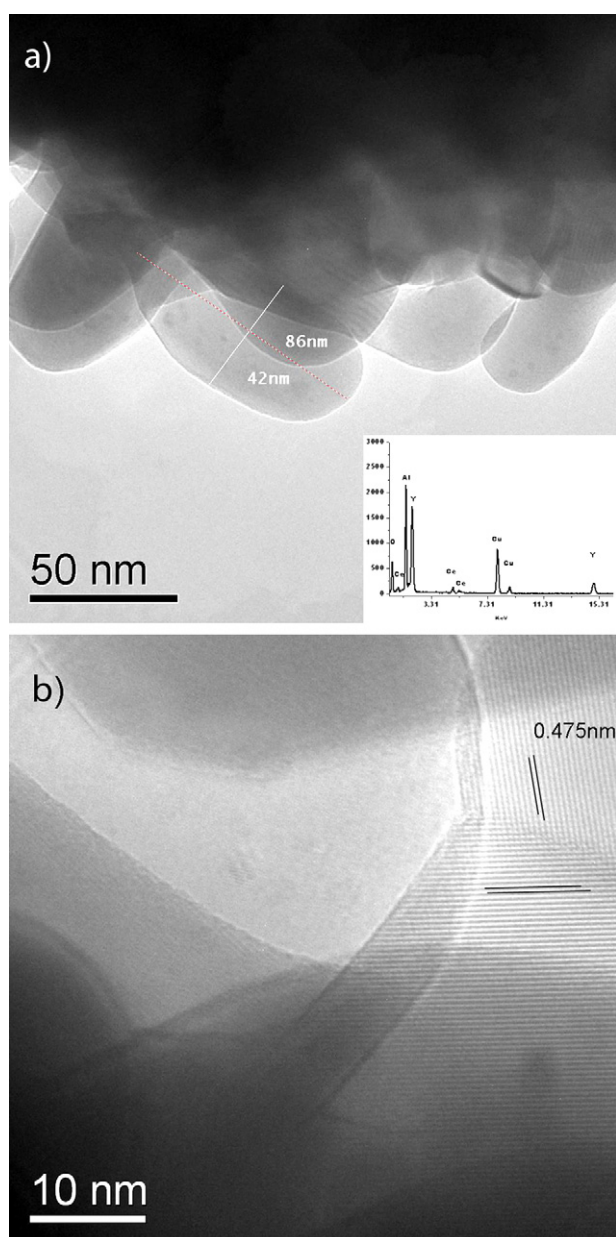


Fig. 4. HRTEM analysis of YAG:Ce³⁺ powders heat treated at 1000 °C (a) and 1100 °C (b).

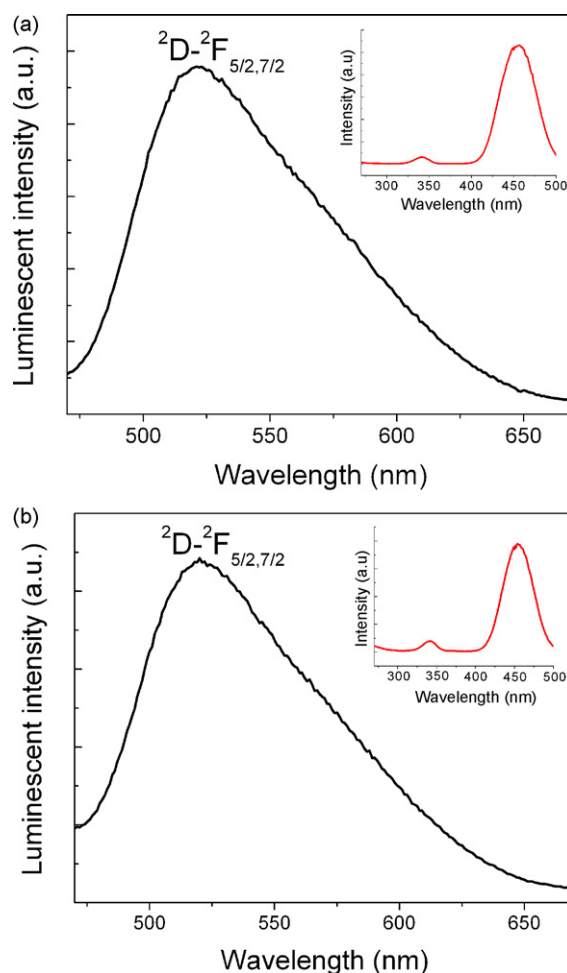


Fig. 5. Photoluminescence emission spectra of YAG:Ce³⁺ powders thermally treated at 1000 °C (a) and 1100 °C (b); the excitation spectra are given as insets.

CeO₂ present as a minority phase in both samples. In accordance to the quantitative Rietveld analysis, CeO₂ content decreases from 9 to 7 wt% with the thermal treatment temperature increase from 1000 to 1100 °C. This is an expectable behaviour since the higher temperature enhances ion diffusivity and influences the accommodation of cerium ions in the garnet matrix. However, the presence of Ce³⁺ in garnet structure is apparent due to the increase of the corresponding bond distances comparing with pure YAG (free of Ce³⁺), Table 1. The correctness of the solution for the proposed YAG:Ce structure is affirmed by good value of the structure relevant reliability factor R_{Bragg} .

SEM analysis of the crystalline YAG:Ce powders are performed to study particle morphology, Fig. 2. It is clear that particles have high sphericity and narrow size distribution. The agglomeration degree is low; only in few cases the clusters comprising several collided particles are observed. According to SEM micrographs, the most of the particles are submicronic in size. On increasing the thermal treatment temperature, the particle surfaces become rougher due to the promoted growth of primary nanoparticles (see insets in Fig. 2), but overall powder morphology reflected through good dispersity remains unchanged. Grained-like surfaces give evidence of composite particle structure and sustained nanoporosity presuming high-specific surface area.

TEM/EDS images of particles thermally treated at 1000 and 1100 °C for 3 h are shown in Fig. 3. It is clear that the particles obtained at different temperatures have similar overall morphology. Comparing to the product obtained from pure nitrate solution^{11,12} where the concentration gradient caused surface precipitation and consequently the hollow particle morphology, here the filled morphology was completely achieved on the account of gelation process within the droplet volume. Corresponding EDS analysis performed individually in each of presented particles confirm the continuous presence of cerium, yttrium, aluminum and oxygen. As it can be seen clearly from Fig. 4, the spherical particles are composed of smaller primary particles that are nanometric in size and elongated, with the longer dimension of 86 nm (Fig. 4(a)). Taking into account that XRD data refinement assumes that the crystallites are approximately equiaxial, the obtained average size of 52 nm for powder treated at the temperature of 1000 °C (Table 1), is in good agreement with the observed one. The primary particles represent randomly oriented monocrystals. Corresponding EDS analysis of monocrystals located at the surfaces of the secondary particles (Fig. 4(a)) confirms homogeneous distribution of all constituent elements, denying the precipitation of CeO₂ phase at the particle surface. Comprehensive microscopic analysis is performed in order to locate the segregated CeO₂ grains but they are not observed. We assume that CeO₂ phase is present in the form of small crystallites which are uniformly distributed through much bigger spherical particles. In accordance to the XRD analysis the calculated size of the CeO₂ crystallites is 23(3) nm in powder thermally treated at 1000 °C. The observed interplanar spacing of 0.475 nm (Fig. 4(b)) and 0.326 nm (Fig. 4(c)) correlates well with the d spacing values of (2 1 1) and (3 2 1) planes of the cubic YAG phase (PDF 33-0040). A high-resolution lattice images imply that the monocrystals

are structurally perfect since no defects are observed within the crystal structure.

The absence of intermediate phases such as YAM, YAP or Y₂O₃, the presence of which we have reported in our previous studies,^{2,12} implies that observed differences in solubility of yttrium and aluminum sources (liable for sequential precipitation and phase segregation) is also overcome through homogeneous dispersion of Y³⁺ and Al³⁺ ions into polymeric organic network formed by esterification.

The emission spectra for the samples annealed at 1000 and 1100 °C are given in Fig. 5, while the excitation spectra are shown as insets in the graphs. It can be noticed that YAG:Ce³⁺ particles absorbed excitation energy in the two different ranges: one from 300 to 370 nm with maximum excitation wavelength near 343 nm (attributed to the host material) and the other excitation range is between 400 and 500 nm with maximum excitation wavelength near 460 nm (attributed to the luminescence centre). For the emission spectra, YAG:Ce³⁺ powders are excited by a xenon lamp operating at a wavelength of 343 nm. When observing the emission spectra it can be noticed that the samples show broad green-yellow emission band in the range of 470–670 nm peaking at 521 nm. In accordance to the literature^{19,20} it is ascribed to the electron transition from the excited state of ²D_J to the ground states of ²F_{5/2,7/2} of Ce³⁺ ions in the Y₃Al₅O₁₂ host material. The overlapping of peak positions in both samples is in agreement with the fact that YAG:Ce³⁺ phases formed at different temperature are structurally similar.

4. Conclusions

In summary, we are able to optimize the spray pyrolysis reaction conditions towards synthesis of pure, unagglomerated YAG:Ce³⁺ particles with spherical shape and filled morphology by introducing the polymer precursor solution (EDTA/EG). The spherical particles comprise grained-like structure, since they are composed of nanosized garnet monocrystals. Although uncompleted, cerium incorporation in garnet matrix is confirmed through XRD, EDS and photoluminescence analyses.

Acknowledgments

This research is financially supported through the Project no. 142010 of the Ministry of Science and Technological Development of Serbia and COST 539 Action. Authors gratefully acknowledge Dr. Vlada Pavlovic, Agricultural Faculty, University of Belgrade for kind assistance in SEM analysis.

References

1. Kang, Y. C., Lenggoro, I. W., Park, S. B. and Okuyama, K., YAG:Ce phosphor particles prepared by ultrasonic spray pyrolysis. *Mater. Res. Bull.*, 2000, **35**, 789–798.
2. Milosevic, O., Mancic, L., Rabanal, M. E., Torralba, J. M., Yang, B. and Townsend, P., Structural and luminescence properties of Gd₂O₃:Eu³⁺ and Y₃Al₅O₁₂:Ce³⁺ phosphor particles synthesized via aerosol. *J. Electrochem. Soc.*, 2005, **152**(9), G707–G713.

3. Psuja, P., Hreniak, D. and Streck, W., Low-voltage cathodoluminescence properties of $\text{Y}_3\text{Al}_5\text{O}_{12}:\text{Tb}^{3+}$ nanopowders. *J. Alloys Compd.*, 2008, **451**(1–2), 571–574.
4. Kinsman, K. M. and McKittrick, J., Phase development and luminescence in chromium doped yttrium aluminum garnet (YAG:Cr) phosphors. *J. Am. Ceram. Soc.*, 1994, **77**(11), 2866–2872.
5. Wang, S., Xu, Y., Lu, P., Xu, C. and Cao, W., Synthesis of yttrium aluminum garnet (YAG) from an ethylenediaminetetraacetic acid precursor. *Mater. Sci. Eng. B*, 2006, **127**, 203–206.
6. Zych, E., Walasek, A. and Szemik-Hojniak, A., Variation of emission color of $\text{Y}_3\text{Al}_5\text{O}_{12}:\text{Ce}$ induced by thermal treatment at reducing atmosphere. *J. Alloys Compd.*, 2008, **451**, 582–585.
7. Li, X., Liu, H., Wang, J., Cui, H. and Han, F., YAG:Ce nano-sized phosphor particles prepared by a solvothermal method. *Mater. Res. Bull.*, 2004, **39**, 1923–1930.
8. Nyman, M., Caruso, J., Hampden-Smith, M. J. and Kodas, T. T., Comparison of solid-state and spray-pyrolysis synthesis of yttrium aluminate powders. *J. Am. Ceram. Soc.*, 1997, **80**(5), 1231–1238.
9. Kang, Y. C., Chung, Y. S. and Park, S. B., Preparation of YAG:europium red phosphors by spray pyrolysis using a filter-expansion aerosol generator. *J. Am. Ceram. Soc.*, 1999, **82**(8), 2056–2060.
10. Purwanto, A., Wang, W.-N., Ogi, T., Lenggono, I. W., Tanabe, E. and Okuyama, K., High luminance YAG:Ce nanoparticles fabricated from urea added aqueous precursor by flame process. *J. Alloys Compd.*, 2008, **463**, 350–357.
11. del Rosario, G., Ohara, S., Mancic, L. and Milosevic, O., Characterisation of YAG:Ce powders thermal treated at different temperatures. *Appl. Surf. Sci.*, 2004, **238**, 469–474.
12. Mancic, L., del Rosario, G., Marinkovic Stanojevic, Z. and Milosevic, O., Phase evolution in Ce-doped yttrium–aluminum-based particles derived from aerosol. *J. Eur. Ceram. Soc.*, 2007, **27**, 4329–4332.
13. Kang, H. S., Kang, Y. C., Park, H. D. and Shul, Y. G., Morphology of particles prepared by spray pyrolysis from organic precursor solution. *Mater. Lett.*, 2003, **57**, 1288–1294.
14. Pebler, A. and Charles, R. G., Synthesis of superconducting oxides by aerosol pyrolysis of metal-edta solutions. *Mater. Res. Bull.*, 1989, **24**, 1069–1076.
15. Lang, R., Ultrasonic atomization of liquids. *J. Acoust. Soc. Am.*, 1962, **34**(1), 6–8.
16. Liu, T. Q., Sakurai, O., Mizutani, N. and Kato, M., *J. Mater. Sci.*, 1986, **21**, 3698–3702.
17. Coelho, A. A., *Topas-Academic*, 2006.
18. Euler, F. and Bruce, J. A., Oxygen coordinates of compounds with garnet structure. *Acta Crystallogr.*, 1965, **19**, 971–978.
19. Yang, H. and Kim, Y.-S., Energy transfer-based spectral properties of Tb-, Pr-, or Sm-codoped YAG:Ce nanocrystalline phosphors. *J. Lumin.*, 2008, **128**, 1570–1576.
20. Blasse, G. and Grabmaier, B. C., *Luminescent Materials*. Springer-Verlag, Berlin, 1994.